

# Optimal reconstruction of the folding landscape using differential energy surface analysis

Arthur La Porta, Natalia A. Denesyuk, and Michel de Messieres  
*University of Maryland College Park, Physics Department,  
 Biophysics Program, Institute for Physical Sciences and Technology*  
 (Dated: July 30, 2012)

In experiments and in simulations, the free energy of a state of a system can be determined from the probability that the state is occupied. However, it is often necessary to impose a biasing potential on the system so that high energy states are sampled with a reasonable frequency. The unbiased energy is typically obtained from the data using the weighted histogram analysis method (WHAM). Here we present differential energy surface analysis (DESA), in which the gradient of the energy surface,  $dE/dx$ , is extracted from data taken with a series of harmonic biasing potentials. It is shown that DESA produces a maximum likelihood estimate of the folding landscape gradient. DESA is used to analyze extension vs. time data taken as an optical trap is used to unfold a DNA hairpin under a harmonic constraint. It is shown that the energy surface obtained from DESA is indistinguishable from the energy surface obtained when WHAM is applied to the same data. Two criteria are defined which indicate whether the DESA results are self-consistent. It is found that these criteria are satisfied for the experimental data analyzed, confirming that data taken with different constraint origins are sampling the same effective energy surface. The combination of DESA and the optical trap assay in which a structure is disrupted under harmonic constraint facilitates an extremely accurate measurement of the folding energy surface.

PACS numbers: 87.14.G-, 87.15.Cc, 87.15.hm

## I. INTRODUCTION

In a dynamical system driven by thermal fluctuations the effective energy  $E$  as a function of conformation  $\mathbf{x}$  is related to the probability  $p$  that the conformation is observed by the Boltzmann formula,

$$p(\mathbf{x}) = \exp\left(\frac{-E(\mathbf{x})}{k_B T}\right), \quad (1)$$

where  $k_B$  is the Boltzmann constant and  $T$  is the temperature. The conformation of a simple system may be specified by a small number of variables. However, in studies of the folding of bio-polymers the conformational space of the system has many degrees of freedom. In some cases, such systems can be described in terms of a single reaction coordinate,  $x$ , and the dynamics of the system can be modeled by diffusion in this 1D space under the influence of an effective energy[1–4]. In numerical simulations the reaction coordinate may be the radius of gyration of the structure, the fraction of native contacts, or another measure of the level of compaction or organization of the molecule. In single molecule manipulation experiments the end-to-end extension of the molecule is typically used as a reaction coordinate[5]. The energy as a function of the reaction coordinate follows from Eq. 1 as

$$E(x) = -k_B T \ln(p(x)) + c. \quad (2)$$

The arbitrary constant  $c$  is included because the energy of a system is only defined up to a additive constant. Although this formula can be used, in principle, to determine the energy surface from the probability density function, this is only practical when the energy varies in a range which is narrow compared with  $k_B T$ . The exponential dependence of the probability density on  $E$  means that states with relative energy that is large compared with  $k_B T$  will be impossible to sample in a finite time.

One solution to this problem is to apply an external force field to the system which tends to bias it towards the regions of the reaction coordinate that would otherwise be poorly sampled. Often, this takes the form of a harmonic constraint, which adds an additional term  $\alpha(x - x_0)^2/2$  to the energy, where  $\alpha$  is the effective stiffness and  $x_0$  is the origin of the constraint. By selecting an appropriate value of  $\alpha$  and varying  $x_0$ , the system can be forced to visit various regions of the reaction coordinate, allowing more uniform convergence of statistics. This technique, often referred to as umbrella sampling[6], is widely used in simulations[7], and has been applied to single molecule experiments[8].

We can still apply Eq. 2 to the system with a specific configuration of the harmonic constraint, but we will obtain a biased energy which is the sum of the intrinsic energy and the energy of the constraint. To find the unbiased energy, we subtract the known constraint energy, and obtain

$$E_j(x) = -k_B T \ln(p_j(x)) - \frac{1}{2}\alpha(x - x_j)^2 + c_j. \quad (3)$$

For each position of the constraint  $x_j$  we obtain a measurement of the energy surface  $E_j(x)$  over the region visited by the system. Each local energy surface  $E_j(x)$  contains an independent constant  $c_j$ .

If we wish to find the global energy surface, defined over the entire domain of  $x$ , we need to choose the constants  $c_j$  and combine the local energy landscapes  $E_j(x)$  in a self-consistent manner. If there is substantial overlap between the domains of the local landscapes, the constants  $c_j$  can be determined by requiring that the energy surfaces corresponding to different constraints are consistent in the overlap regions.

The weighted histogram analysis method (WHAM) has been formulated to reconstruct the energy surface  $E(x)$  from Monte Carlo or molecular dynamics simulations with arbitrary biasing potentials[9–12]. The method provides an op-

timal estimate for the unbiased probability density  $p(x)$ ,

$$p(x) = \sum_i p_i(x) w_i(x), \quad (4)$$

where  $p_i(x)$  is the probability density sampled in biased simulation  $i$  and the summation is over all simulations. In the case of a harmonic constraint centered at  $x_i$ , the weights  $w_i(x)$  are given by

$$w_i(x) = \frac{M_i}{\sum_j M_j \exp \left[ f_j - \frac{\alpha(x - x_j)^2}{2k_B T} \right]}, \quad (5)$$

where  $M_i$  is the total number of measurements in simulation  $i$ . The constants  $f_i$  are defined implicitly by a system of non-linear equations,

$$\exp(-f_i) = \int dx \exp \left( -\frac{\alpha(x - x_i)^2}{2k_B T} \right) \times \frac{\sum_j \frac{H_j(x)}{dx}}{\sum_k M_k \exp \left[ f_k - \frac{\alpha(x - x_k)^2}{2k_B T} \right]}, \quad (6)$$

where the histogram count  $H_j(x)$  is the number of measurements between  $x$  and  $x + dx$  in system  $j$ , and is related to the probability by  $p_j(x)dx = H_j(x)/M_j$ .

In the following section, we describe another method of obtaining the global energy surface which we call differential energy surface analysis (DESA). In DESA, we consider the slope of the energy landscape,  $dE/dx$  rather than the energy itself. Differentiating Eq. 3 with respect to  $x$  we obtain

$$\frac{dE_j}{dx}(x) = -k_B T \frac{d}{dx} [\ln(p_j(x))] - \alpha(x - x_j). \quad (7)$$

An important feature of this equation is that the constants  $c_j$  are eliminated, so that it is not necessary to find a self-consistent solution to obtain the global function  $dE/dx$ . At any given point  $x$  along the landscape,  $dE/dx$  can be obtained by averaging  $dE_j/dx$  obtained from the system at various constraint origins.

## II. DESCRIPTION OF DESA

In order to define the method of differential energy landscape analysis, we assume a thermally driven system with one reaction coordinate  $x$  which is characterized by an energy function  $E(x)$ . We assume that the dynamics of the system are measured in the presence of a harmonic constraint of stiffness  $\alpha$  for  $N$  distinct constraint origins  $x_j$ . For each  $x_j$ , the time series of  $x$  is used to compile a histogram  $H_j(x_i)$  containing  $M_j$  total samples. We assume that the histogram binning is consistent for all  $x_j$ , and that the values of  $\alpha$  and  $x_j$  are chosen so that there is significant overlap between the histograms. The slope of the energy landscape  $dE/dx$  at position

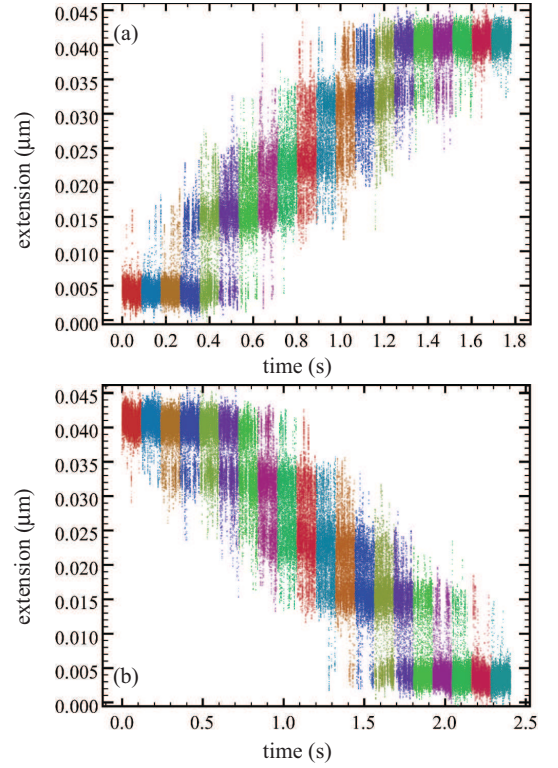


FIG. 1. The extension of a DNA hairpin as a function of time as the constraint origin is moved. In (a) the hairpin is initially closed and the constraint moves at 25 nm/s. In (b) the hairpin is initially open and the constraint moves at  $-25$  nm/s.

$x_i$  is given by

$$\frac{dE}{dx}(x_i) = \frac{\sum_j H_j(x_i) \frac{dE_j}{dx}(x_i)}{\sum_j H_j(x_i)}, \quad (8)$$

where the summation is over the constraint origins,  $x_j$ , and  $\frac{dE_j}{dx}(x_i)$  is defined by Eq. 7. Interpreting this formula, the value of  $dE/dx$  at position  $x_i$  is a weighted average of  $dE_j/dx$  found from the  $N$  systems with constraint origins  $x_j$ . Using  $p_j(x_i)\Delta x = H_j(x_i)/M_j$ , we can express Eq. 8 entirely in terms of histogram counts, as

$$\frac{dE}{dx}(x_i) = \frac{\sum_j [-k_B T \frac{d}{dx} (\ln H_j(x_i)) - \alpha(x_i - x_j)] H_j(x_i)}{\sum_j H_j(x_i)}. \quad (9)$$

This formula has been used to reconstruct energy landscapes of molecular dynamics simulations[13], and experimental data[8]. We will show below that Eq. 9 gives an optimal estimation of  $dE/dx$ .

When determining the mean value of a variable from data points which have differing uncertainty, the maximum likelihood solution is

$$\bar{a} = \frac{\sum_i w_i a_i}{\sum_i w_i}, \quad \sigma_a^2 = \frac{1}{\sum_i w_i}, \quad w_i = \frac{1}{\sigma_i^2}, \quad (10)$$

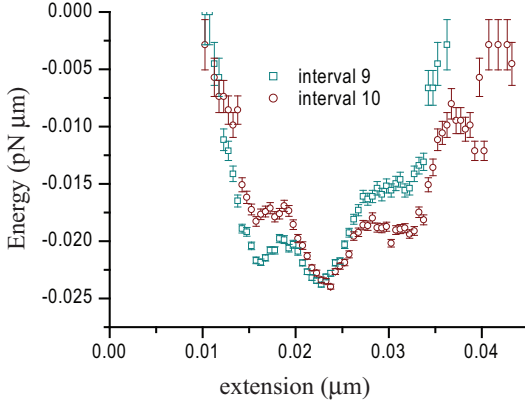


FIG. 2. The biased energy of the hairpin, as calculated from data in intervals 9 and 10 of Fig. 1(a) using Eq. 2.

where  $\sigma_i$  is the standard deviation of the statistical ensemble from which  $a_i$  is taken,  $\bar{a}$  is the mean of  $a$  and  $\sigma_{\bar{a}}$  is the standard deviation of  $\bar{a}$ . In order to show that Eq. 8 is a maximum likelihood estimate of  $dE/dx$  we must show that the choice  $w_j(x_i) = H_j(x_i)$  meets the criteria set out in Eq. 10.

Starting with Eq. 7, the evaluation of  $dE/dx$  will involve a finite difference of the natural logarithm of  $H_j(x_i)$ ,

$$\frac{dE_j}{dx}(x_i) = \frac{-k_B T}{\Delta x} [\ln(H_j(x_{i+1}) \pm \Delta H_j(x_{i+1})) - \ln(H_j(x_i) \pm \Delta H_j(x_i))], \quad (11)$$

where  $\Delta H_j(x_i)$  represents the statistical uncertainty in  $H_j(x_i)$ , and  $\Delta x = x_{i+1} - x_i$ . We can re-express Eq. 11 as

$$\begin{aligned} \frac{dE_j}{dx}(x_i) &= \frac{k_B T}{\Delta x} \left[ \ln \left( H_j(x_{i+1}) \left( 1 \pm \frac{\Delta H_j(x_{i+1})}{H_j(x_{i+1})} \right) \right) \right. \\ &\quad \left. - \ln \left( H_j(x_i) \left( 1 \pm \frac{\Delta H_j(x_i)}{H_j(x_i)} \right) \right) \right] \\ &= \frac{k_B T}{\Delta x} \left[ \ln(H_j(x_{i+1})) - \ln(H_j(x_i)) \right. \\ &\quad \left. + \ln \left( 1 \pm \frac{\Delta H_j(x_{i+1})}{H_j(x_{i+1})} \right) \right. \\ &\quad \left. - \ln \left( 1 \pm \frac{\Delta H_j(x_i)}{H_j(x_i)} \right) \right], \quad (12) \end{aligned}$$

so that the uncertainties in  $H_j(x_i)$  and  $H_j(x_{i+1})$  produce additive uncertainties in  $dE_j/dx$ . Assuming the uncertainty in  $H_j(x_i)$  is statistical, the uncertainty terms can be simplified using  $\Delta H_j(x_i) = \sqrt{H_j(x_i)}$ , so that

$$\ln \left( 1 \pm \frac{\Delta H_j(x_i)}{H_j(x_i)} \right) = \ln \left( 1 \pm \frac{\sqrt{H_j(x_i)}}{H_j(x_i)} \right) \approx \frac{\pm 1}{\sqrt{H_j(x_i)}}, \quad (13)$$

where the last step is an expansion of the expression to first order. Since  $\Delta H_j(x_i)$  and  $\Delta H_j(x_{i+1})$  are uncorrelated, the errors arising from these terms add in quadrature. In the limit that  $\Delta x$  is small we can neglect the difference between  $H_j(x_i)$

and  $H_j(x_{i+1})$ , and using Eq. 13 approximate the uncertainty in  $\frac{dE_j}{dx}$  as

$$\sigma = \frac{k_B T \sqrt{2}}{\Delta x \sqrt{H_j(x_i)}}. \quad (14)$$

The statistical weight required for maximum likelihood is therefore

$$w_j(x_i) = \frac{1}{\sigma^2} = \left( \frac{\Delta x}{k_B T} \right)^2 \frac{H_j(x_i)}{2}. \quad (15)$$

Since an overall multiplicative factor will cancel out in Eq. 10 and not affect the calculation of the mean value, Eq. 8 is equivalent to the maximum likelihood estimation of  $dE/dx$  and is an optimal estimation.

### III. APPLICATION OF DESA TO EXPERIMENTAL DATA

The weighted histogram analysis method (WHAM) produces an optimal estimation of  $p$ , which is closely related to  $E$ , and differential energy surface analysis (DESA) produces an optimal estimation of  $dE/dx$ . If data is statistically well converged, and collected from a system that thoroughly samples its equilibrium ensemble, both DESA and WHAM will converge to the same underlying energy landscape. However, in experiments and in simulations, it is often a challenge to obtain adequate statistical convergence or to verify that the equilibrium ensemble has been adequately sampled. It is interesting to consider the accuracy of DESA, and whether it produces results which are significantly different from those produced by WHAM in cases where convergence of statistics is less than ideal.

We will apply DESA and WHAM to single molecule experiment in which a DNA hairpin is unfolded under a harmonic constraint applied by an optical trap. The hairpin has sequence CCGCGAGTTGATTCGCCATACACCTGCTAATCCCGGTCGCTTTTTCGACCGGGATTAGCAGGTGTATGGCGAATCAACTCGCGG, which folds into a 40 base-pair stem with a 4-T loop. It is connected to the boundary of the sample chamber on one side and to a polystyrene micro-sphere on the other via biotin and digoxigenin tagged double-stranded DNA linkers. When the optical trap is held at constant position and intensity, the combination of the restoring force imposed on the micro-sphere by the optical trap and the elasticity of the handles produce a harmonic constraint acting on the hairpin with  $\alpha \approx 200$  pN/ $\mu$ m. The position of the sample chamber is controlled by a piezoelectric positioning stage with nanometer resolution, and the origin of the constraint is controlled by varying the position of the sample chamber with respect to the trap center. The optical trap measures the instantaneous position of the micro-sphere and instantaneous force applied to the tether as the constraint origin is swept. By determining the total length of the tether and subtracting off the instantaneous extension of the double-stranded DNA handles (estimated using a worm-like chain model of DNA elasticity) the extension

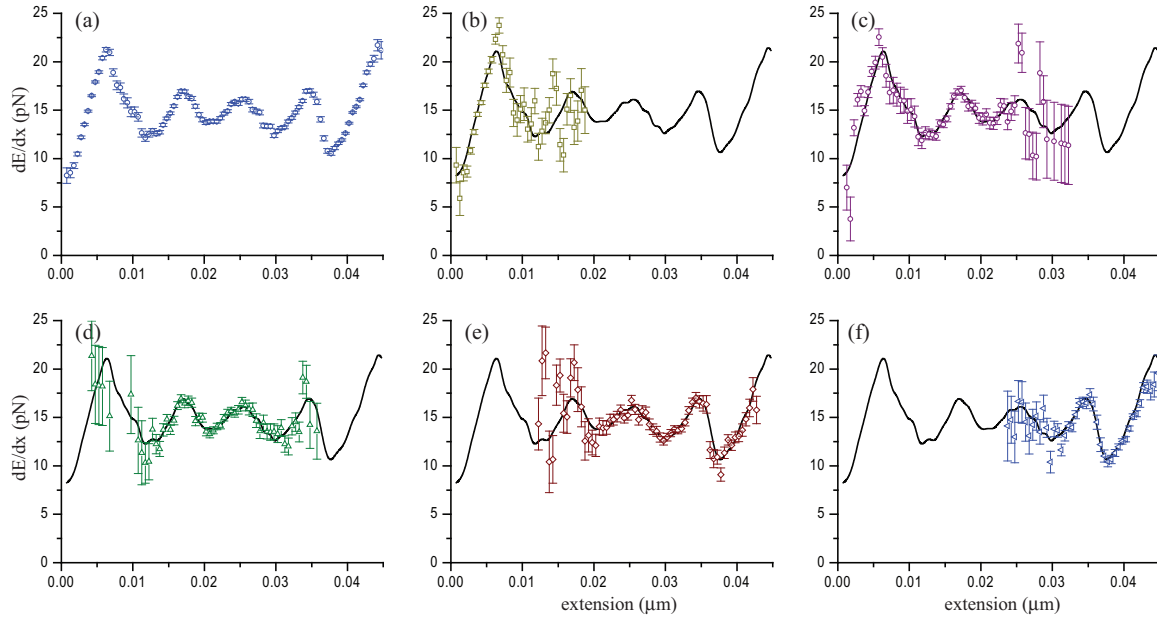


FIG. 3. (a) Reconstructed  $dE/dx$  plot. In (b)-(f) the  $dE_j/dx$  estimates from the 3rd, 6th, 9th, 12th and 15th intervals are compared with the reconstructed  $dE/dx$  function. The  $dE_j/dx$  values are calculated using Eq. 7. For (a) the uncertainty is based on the maximum likelihood result given in Eq. 10 for (b)-(f) uncertainty is based on Eq. 12.

of the hairpin itself is determined[14]. The apparatus and experimental procedure has been described elsewhere[8]. The measured time series comprised of approximately  $10^5$  samples is shown for unfolding of the hairpin in Fig. 1(a), and for folding of the hairpin in Fig. 1(b).

The record of extension vs. time of the experimental system is divided into 20 equal time intervals and the histogram of position is calculated for each interval. Calibration data is used to calculate the mean stiffness and origin of the constraint for each of the 20 intervals. Since the constraint origin moves continuously as data is acquired, it is not a constant within each interval. However, the deviation of the constraint origin from the mean value does not exceed  $\sim 1$  nm in the course of an interval, which implies an error in the constraint correction of less than  $\sim 0.2$  pN. Therefore analysis of each interval using the mean constraint origin is a negligible source of error.

The biased energy surfaces obtained by applying Eq. 2 to the histograms compiled from two adjacent intervals in Fig. 1(a) are shown in Fig. 2. The underlying potential, due to the sequence dependence of the hairpin stem hybridization energy, is the same for the two histograms shown, but the broad parabolic potential of the constraint shifts slightly as the constraint origin is moved. The purpose of DESA (or WHAM) is to compensate for the effect of the harmonic constraint and extract the shape of the underlying energy surface.

In Fig. 3 the averaged  $dE/dx$  function calculated from the data in Fig. 1(a) is shown. In panels (b) through (f), 5 representative  $dE_j/dx$  functions (calculated by applying Eq. 7 to individual histograms) are selected from the 20 functions used to compute the averaged function. Examining the  $dE_j/dx$  plots, each covers a different domain of the extension and ex-

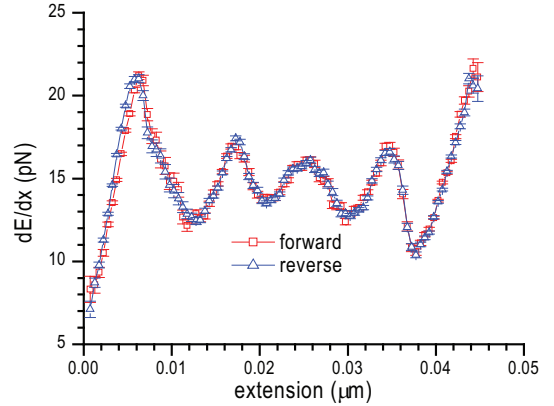


FIG. 4. The  $dE/dx$  curves obtained from unfolding and folding of the hairpin are compared.

hibits low uncertainty near the center of the domain, where statistics are well converged, and high uncertainty near the margins of the domain. The individual  $dE_j/dx$  functions are consistent with the average  $dE/dx$  within experimental uncertainty. The energy of the hairpin as a function of extension is not known *a priori*, but the individual  $dE_j/dx$  curves are consistent with the average  $dE/dx$  function, and with each other. The fact that all 20 of the individual  $dE_j/dx$  functions (a subset of which is shown in Fig. 3) agree with the average function is evidence that the same underlying landscape is being measured for all 20 constraint origins, and that the system has not jumped to a different branch of the energy landscape as the constraint is moved. In Supplemental appendix

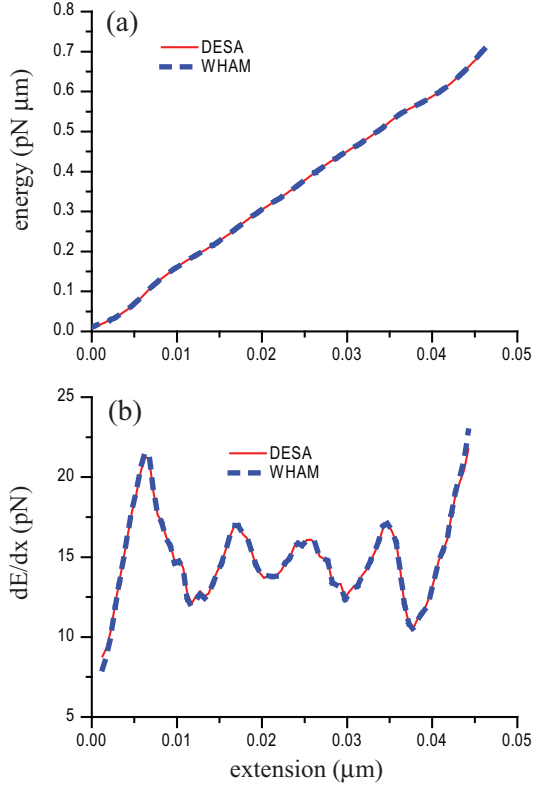


FIG. 5. (a) Comparison of the energy surface obtained by DESA and by WHAM from the time series in Fig. 1(a). (b) Comparison of  $dE/dx$  obtained by DESA and WHAM from the time series in Fig. 1(a).

Figs. S2 and S3, DESA is applied to a simulated system for which the energy surface is known, allowing direct confirmation that DESA produces the correct  $dE/dx$  function.

In the umbrella sampling method, it is assumed that the biasing potential is time independent and that the system is in thermodynamic equilibrium as data is collected. In our experiment the constraint origin moves continuously as data is acquired and analyzing the data using the DESA or WHAM involves an approximation. The most convincing evidence that the system remains in effective equilibrium as the constraint origin moves is that identical energy landscapes are obtained for folding and unfolding of the hairpin, for which the constraint origin moves in opposite directions. The energy landscapes obtained from data in Figs. 1(a) and 1(b) are compared in Fig. 4. No significant difference is found between landscapes obtained for folding and unfolding of the hairpin.

There are systems, such as pseudoknots, G-quadruplex DNA and others, which exhibit large irreversible steps when disrupted in single molecule experiments[15, 16]. In such cases, the techniques described here would not be suitable for reconstructing the global energy landscape. Nonequilibrium analysis methods have been developed which can determine the energy surface from data taken far from equilibrium[17–22]. These methods typically require a great deal of experimental data, since they involve measuring the dependence of

the disruption force on force loading rate or averaging many trajectories with weights determined by the external work performed. In cases where a molecule can be disrupted progressively in a reversible manner, we find it advantageous to employ equilibrium methods, which requires only a single trajectory.

In order to verify the DESA result, the data shown in Fig. 1 was also analyzed using WHAM, as defined by Eqs 5 and 6. In Fig. 5(a) the energy surface obtained by WHAM is plotted along with the energy surface obtained from integration of the  $dE/dx$  curve shown in Fig. 3. The DESA and WHAM curves are indistinguishable. The overall slope of the energy landscape is reproduced, as well as the ripples that arise from the sequence dependence of the DNA hybridization energy. The sequence dependence is more apparent in the plot of  $dE/dx$ , which is shown in Fig. 5(b). As in the case of the energy, results obtained from DESA and WHAM are indistinguishable.

#### IV. DIAGNOSTICS IN THE DESA METHOD

Recent work has provided criteria for error estimation in free energy calculations based on the weighted histogram analysis method[23, 24]. The DESA result is obtained by straightforward averaging of  $dE_j/dx$  estimates obtained from different constraint origins. Use of the maximum likelihood estimation assures that the optimal value of  $dE/dx$  is produced, and straightforward error propagation can be used to obtain the uncertainty in the values of  $dE/dx$  obtained. However, when employing umbrella sampling, it is necessary to assume that the data acquired with different constraint origins is sampling the same energy surface. One potential pitfall of the DESA method is that we can obtain a smooth average  $dE/dx$  curve, even if the system jumps to a different energy surface as the constraint origin is moved. Here we introduce two criteria that can be applied in order to detect inconsistencies in  $dE_j/dx$  values obtained from different constraint origins and we illustrate the results obtained when these criteria are applied to experimental data.

The first method involves comparison of the biased energy surfaces obtained from different constraint origins. Subtracting two biased energies, we obtain

$$\begin{aligned}
 E_{b,k}(x) - E_{b,j}(x) &= \\
 & \left[ E_{\text{hp}}(x) + \frac{\alpha}{2}(x - x_k)^2 \right] - \left[ E_{\text{hp}}(x) + \frac{\alpha}{2}(x - x_j)^2 \right] \\
 &= x [\alpha(x_j - x_k)] + \frac{\alpha}{2} (x_k^2 - x_j^2), \quad (16)
 \end{aligned}$$

where  $E_{b,j}(x)$  is the biased energy surface measured with constraint origin  $x_j$  and  $E_{\text{hp}}(x)$  is the intrinsic energy of the hairpin. The cancelation of  $E_{\text{hp}}(x)$  leaves terms which depend only on the biasing potential. The constant term is not of interest, since the energy itself is only defined up to an additive constant. However, we expect the energy difference to manifest a straight line with slope determined by the constraint strength and the relative constraint displacement,  $\alpha(x_j - x_k)$ . If a different effective energy surface is in effect after the constraint origin is moved,  $E_{\text{hp}}$  will fail to cancel in Eq. 6 and



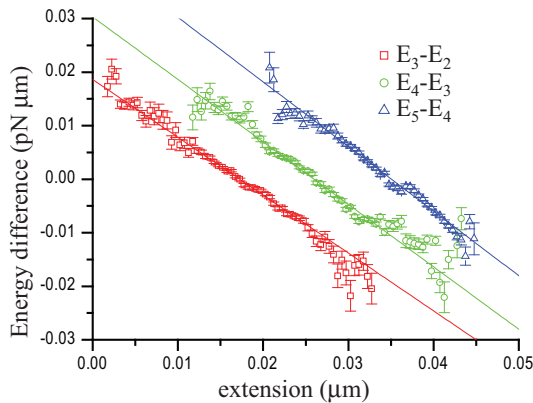


FIG. 6. The difference in biased energy for adjacent intervals. Data is as in Fig. 2 except the time series is divided into six intervals rather than twenty. The differences  $E_3(x) - E_2(x)$ ,  $E_4(x) - E_3(x)$  and  $E_5(x) - E_4(x)$  are shown.

anomalous features will appear in the difference curve.

Applying this criteria to the single molecule experiment, we recompiled the histograms from the data shown in Fig. 1(a) using 6 intervals rather than 20 (to improve statistical convergence) and subtracted the biased energy surfaces for adjacent intervals. The result is shown in Fig. 6. The fact that straight lines with the expected slope are found are strong evidence that the  $E_{hp}$  effective at different constraint origins have canceled, as expected, and that the  $dE/dx$  values being averaged are mutually consistent.

We can also test the self-consistency of the DESA analysis by determining if  $dE_j/dx$  values obtained from individual constraint origins deviate from the mean value in a manner that is consistent with their statistical uncertainty. When considering Fig. 3 above, it was observed that individual  $dE_j/dx$  curves appear to be mutually consistent and values typically fall within a standard deviation of the mean value. This criteria can be expressed more rigorously using a simple reduced

$\chi^2$  test. For each histogram bin  $i$ , we evaluate

$$\chi^2 = \frac{1}{N-1} \sum_j \frac{\left( \frac{dE_j}{dx} - \frac{dE}{dx} \right)^2}{\sigma_j^2}, \quad (17)$$

where  $\sigma_j$  is the uncertainty in the value of  $\frac{dE_j}{dx}$  obtained from the  $j^{\text{th}}$  constraint position. If the deviation of the individual values of  $dE_j/dx$  are consistent with the statistical uncertainty, the value of  $\chi^2$  should be of order 1. A value significantly larger than 1 indicates that systematic errors are present in the  $dE_j/dx$  values.

In Fig. 7 the value of the reduced  $\chi^2$  is plotted as a function of extension for the experimental data set. For the central portion of the extension range, the  $\chi^2$  values are of order unity, indicating that the DESA method is working as expected. However, for the extremes of extension, the  $\chi^2$  values are higher, which would indicate that contributions from different constraint origins are not consistent. This can be attributed to the fact measurement uncertainty becomes more significant when the hairpin is fully extended or fully folded.

When the constraint origin is positioned to stabilize the hairpin in the fully open or fully closed conformation, the conformational dynamics of the hairpin itself are minimal and the fluctuations in the measured extension are largely due to thermal fluctuations in the handles. At small extension, the problem is compounded by the fact that the average force is low, resulting in lower stiffness of the handles and increased fluctuations. These measurement errors blur the sharp cut-off that would otherwise appear in the probability density as the hairpin reaches the fully-open or fully-folded state, and similarly blur the energy function. The  $\chi^2$  function alerts us to the fact that the energy surface is accurately measured in the central part of the unfolding range, but that if affected by systematic errors near the fully folded or fully unfolded state. (For comparison, the  $\chi^2$  test is applied to simulated data in Supplemental appendix Fig. S4.) This illustrates how the  $\chi^2$  criteria can be an effective way of evaluating the quality of the DESA determination of  $dE/dx$  as a function of the reaction coordinate.

## V. CONCLUSIONS

We have described the differential energy landscape analysis method, and shown that it is an optimal estimation of  $dE/dx$ . This is complementary to the weighted histogram method, which gives an optimal estimation of  $p$ . We have demonstrated the application of the DESA technique to single molecule experimental data and have shown that DESA and WHAM produce indistinguishable results when applied to the same data. DESA is defined by a formula that can be written in closed form (Eq. 8) and is computationally simpler than WHAM, which requires the self-consistent solution of a system of nonlinear equations (Eq. 6). To apply DESA we must assume that the system is sampling the same branch of the folding energy surface as the constraint origin is moved. We have described two criteria for determining

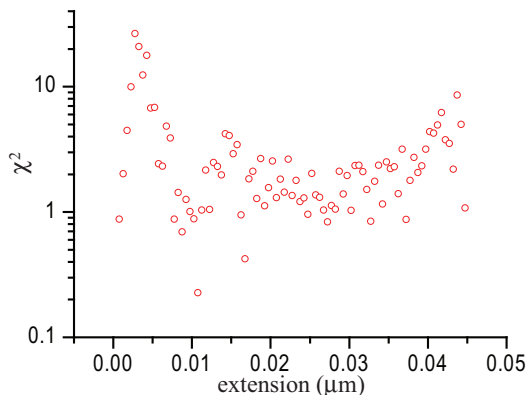


FIG. 7. The value of  $\chi^2$  as a function of extension, for the data shown in Fig. 1(a).

whether the  $dE/dx$  data obtained by application of DESA are self-consistent, which can be used to validate this assumption. Our experimental system is formally out of equilibrium, since the constraint origin is moved continuously as data is acquired. However, equilibrium techniques provide an accurate measurement of the landscape in this case because the rate at

which the constraint is moved is slow compared with the rate at which the system equilibrates. This is attributable to the fact that no high energy barriers are present in the biased energy landscape as the constraint origin is swept.

This work was supported by the Maryland Technology Development Corporation.

- 
- [1] S. S. Plotkin and J. N. Onuchic, *Quarterly Reviews of Biophysics* **35**, 111 (2002).
  - [2] J. N. Onuchic and P. G. Wolynes, *Current Opinion in Structural Biology* **14**, 70 (2004).
  - [3] P. G. Wolynes, J. N. Onuchic, and D. Thirumalai, *Science* **267**, 1619 (1995).
  - [4] K. A. Dill, S. B. Ozkan, M. S. Shell, and T. R. Weikl, *Annual Reviews of Biophysics* **37**, 289 (2008).
  - [5] J. Liphardt, B. Onoa, S. B. Smith, I. Tinoco, and C. Bustamante, *Science* **292**, 733 (2001).
  - [6] G. M. Torrie and J. P. Valleau, *Chemical Physics Letters* **28**, 578 (1974).
  - [7] D. Frenkel and B. Smit, *Understanding Molecular Simulation* (Academic Press, 2003).
  - [8] M. de Messieres, B. Brawn-Cinani, and A. La Porta, *Biophysical Journal* **100**, 2736 (2011).
  - [9] H. A. Kramers, *Physica* **VII**, 284 (1940).
  - [10] A. M. Ferrenberg and R. H. Swendsen, *Physical Review Letters* **63**, 1195 (1989).
  - [11] S. Kumar, J. M. Rosenberg, D. Bouzide, R. H. Swendsen, and P. A. Kollman, *Journal of Computational Chemistry* **13**, 1011 (1992).
  - [12] E. M. Boczek and C. L. Brooks, *Science* **269**, 393 (1995).
  - [13] N. A. Denesyuk and J. D. Weeks, *Physical Review Letters* **102**, 108101 (2009).
  - [14] J. Marko and E. Siggia, *Macromolecules* **28**, 8759 (1995).
  - [15] L. Green, C.-H. Kim, C. Bustamante, and J. Tinoco, *Journal of Molecular Biology* **375**, 511 (2008).
  - [16] Z. Yu, J. D. Schonhort, S. Dhakal, R. Bajracharya, R. Hegde, S. Basu, and H. Mao, *Journal of the American Chemical Society* **131**, 1876 (2009).
  - [17] C. Jarzynski, *Physical Review Letters* **78**, 2390 (1997).
  - [18] G. E. Crooks, *Phys. Rev. E* **61**, 2361 (2000).
  - [19] G. Hummer and A. Szabo, *PNAS* **98**, 3658 (2001).
  - [20] G. Hummer and A. Szabo, *PNAS* **107**, 21441 (2010).
  - [21] E. Evans, *Annual Review of Biophysics and Biomolecular Structure* **30**, 105 (2001).
  - [22] O. K. Dudko, G. Hummer, and A. Szabo, *Proceedings of the National Academy of Science* **105**, 15755 (2008).
  - [23] R. Zhu and G. Hummer, *Journal of Computational Chemistry* **33**, 453 (2011).
  - [24] J. D. Chodera, W. C. Swope, J. W. Pitera, C. Seok, and K. A. Dill, *Journal of Chemical Theory and Computation* **3**, 26 (2007).

# Optimal reconstruction of the folding landscape using differential energy surface analysis - SI appendix

Arthur La Porta, Natalia A. Denesyuk and Michel de Messieres

In the body of the paper we apply DESA and WHAM a data set collected in an single molecule experiment. For comparison, we present a Langevin simulation of a strongly damped particle moving in a one dimensional potential specified by a forth order polynomial. The polynomial was chosen to be qualitatively similar to the folding energy of the hairpin. In the main body of the paper DESA is applied to an experimental system which includes such practical challenges as calibration uncertainty, instrumental noise and the finite time resolution of the apparatus. The simulated system is less complex, but has the advantage that the results obtained from DESA can be compared with the known energy surface.

The Langevin simulation uses effective energy  $E(x) = a(x - x_0)^4 + b(x - x_0)^2 + c(x - x_0)$ , where  $x_0 = 0.025 \mu\text{m}$ ,  $a = 1.024 \times 10^6 \text{ pN}/\mu\text{m}^3$ ,  $b = 320 \text{ pN}/\mu\text{m}$ , and  $c = 2.5 \text{ pN}$ . This landscape is plotted in Fig. S1 and has one stable state and one metastable state separated from the stable state by a shallow barrier. If this system is simulated directly it will remain in the stable 'closed' state. In analogy with the experimental system, a harmonic constraint with stiffness  $500 \text{ pN}/\mu\text{m}$  is imposed on the

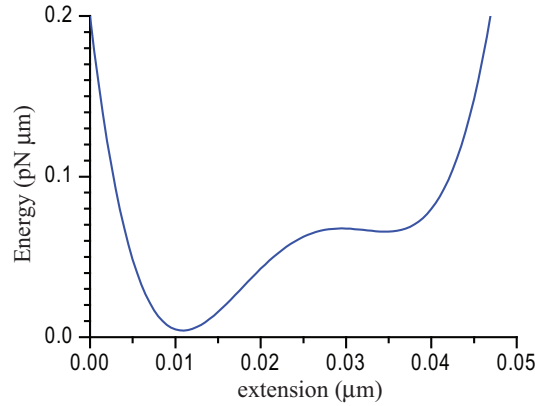


Figure S1: The energy function used in the Langevin simulation.



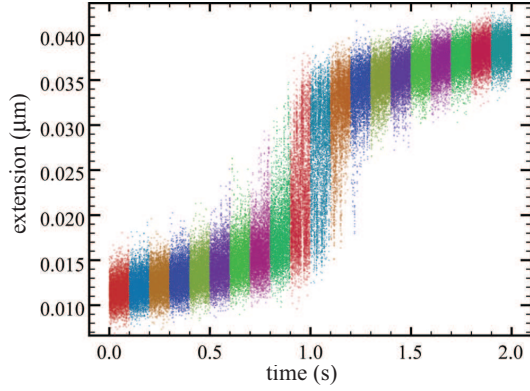


Figure S2: The coordinate of the simulated system as a function of time as the constraint origin is moved from at 17.5 nm/s.

system. In order to match the apparent time scale of the simulation to the experimental data, the effective drag on the particle chosen to be  $0.05 \text{ pN} \cdot \text{s}/\mu\text{m}$ , and 400 substeps of  $5 \times 10^{-8} \text{ s}$  were taken between data samples using  $k_B T = 4.114 \times 10^{-3} \text{ pN} \cdot \mu\text{m}$ . The constraint origin was swept from  $0.0125 \mu\text{m}$  to  $0.0475 \mu\text{m}$  during the course of 2 seconds, producing a time series of  $10^5$  samples. The measured time series is shown in Fig. S2.

In Fig. S3 the averaged  $dE/dx$  function, calculated from the simulated data in Fig. S2, is shown and compared with  $dE/dx$  of the theoretical energy function. Agreement between the DESA result and the theoretical curve is consistent with the statistical uncertainty in the averaged function. In panels (b) through (f), 5 representative  $dE_j/dx$  functions are selected from the 20 functions used to compute the averaged function. Examining the individual  $dE_j/dx$  plots, each covers a different domain of the extension and exhibits low uncertainty near the center of the domain, where statistics are well converged, and high uncertainty near the margins of the domain. The individual  $dE_j/dx$  functions are consistent with the theoretical  $dE/dx$  within experimental uncertainty. A similar relationship between the individual  $dE_j/dx$  and the average  $dE/dx$  is observed in the experimental data shown in the main body of the paper. The fact that the energy in the simulation is known *a priori* allows a rigorous evaluation of the results of the DESA method.

The  $\chi^2$  measure defined in the main manuscript is shown for the experimental and simulated system in Fig. S4. The simulated system gives  $\chi^2$  of order 1, as expected. The experimental system behaves in a similar way for the central portion of the reaction coordinate, but exhibits systematic error for large and small extension, as discussed in the main text.

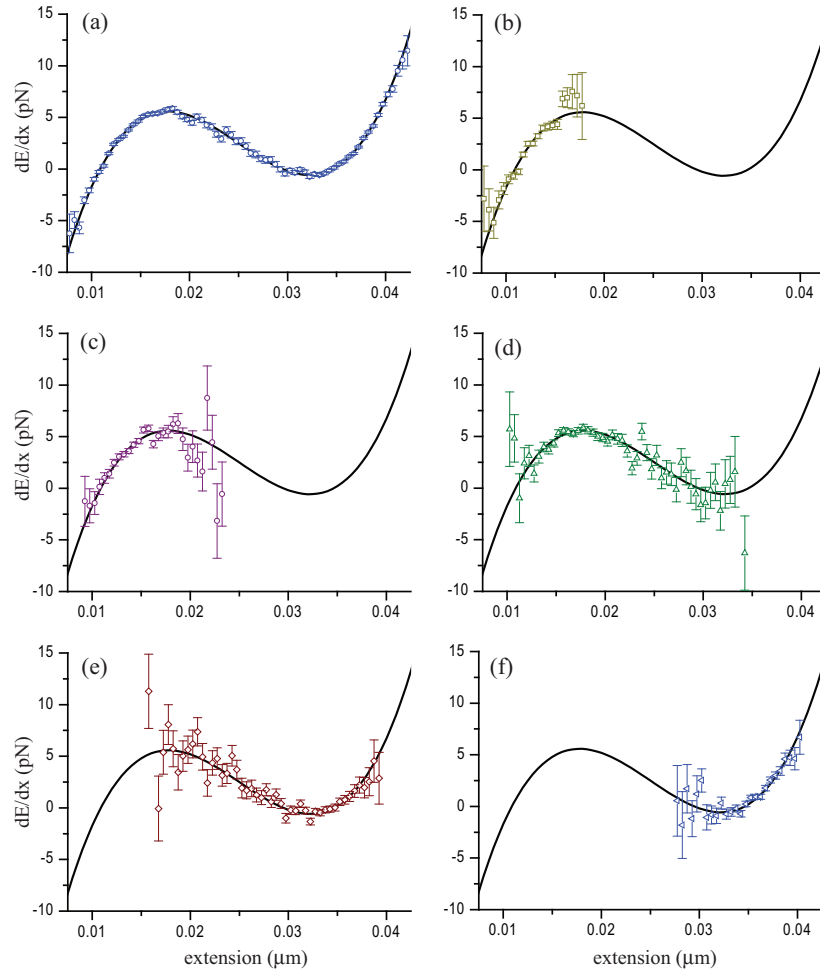


Figure S3: (a) Reconstructed  $dE/dx$  plot of the simulated system in Fig. S2. In (b)-(f) the  $dE_j/dx$  estimate from the 3rd, 6th, 9th, 12th and 15th interval are compared with the reconstructed  $dE/dx$  function.

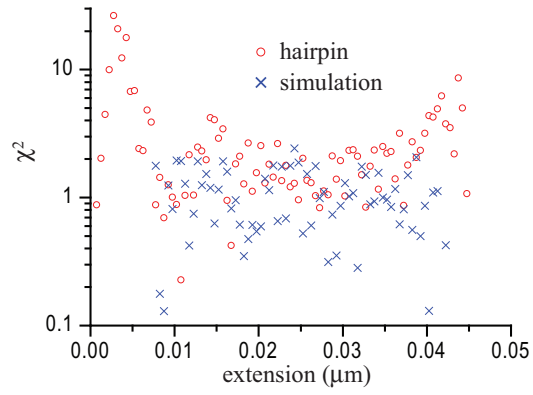


Figure S4: The value of  $\chi^2$  as a function of extension, for the experimental system considered in the body of the paper and for the simulation.